

Published in final edited form as:

Biochemistry. 2002 June 18; 41(24): 7841–7848.

## Characterization of a Novel Mammalian Phosphatase Having Sequence Similarity to *Schizosaccharomyces pombe* PHO2 and *Saccharomyces cerevisiae* PHO13<sup>†</sup>

MacKevin I. Ndubuisi<sup>†,§</sup>, Benjamin H. B. Kwok<sup>†,§</sup>, Jonathan Vervoort<sup>§</sup>, Brian D. Koh<sup>§</sup>, Mikael Elofsson<sup>§,||</sup>, and Craig M. Crews<sup>\*,§,⊥, #</sup>

<sup>§</sup>Department of Molecular, Cellular and Developmental Biology, Yale University, New Haven, Connecticut 06520-8103

<sup>⊥</sup>Department of Pharmacology, Yale University, New Haven, Connecticut 06520-8103

<sup>#</sup>Department of Chemistry, Yale University, New Haven, Connecticut 06520-8103

### Abstract

p34, a specific *p*-nitrophenyl phosphatase (pNPPase) was identified and purified from the murine cell line EL4 in a screen for the intracellular molecular targets of the antiinflammatory natural product parthenolide. A BLAST search analysis revealed that it has a high degree of sequence similarity to two yeast alkaline phosphatases. We have cloned, sequenced, and expressed p34 as a GST-tagged fusion protein in *Escherichia coli* and an EE-epitope-tagged fusion protein in mammalian cells. Using *p*-nitrophenyl phosphate (pNPP) as a substrate, p34 is optimally active at pH 7.6 with a  $K_m$  of 1.36 mM and  $K_{cat}$  of 0.052 min<sup>-1</sup>. Addition of 1 mM Mg<sup>2+</sup> to the reaction mixture increases its activity by 14-fold. Other divalent metal ions such as Co<sup>2+</sup> and Mn<sup>2+</sup> also stimulated the activity of the enzyme, while Zn<sup>2+</sup>, Fe<sup>2+</sup>, and Cu<sup>2+</sup> had no effect. Furthermore, both NaCl and KCl enhanced the activity of the enzyme, having maximal effect at 50 and 75 mM, respectively. The enzyme is inhibited by sodium orthovanadate but not by sodium fluoride or okadaic acid. Mutational analysis data suggest that p34 belongs to the group of phosphatases characterized by the sequence motif DXDX(T/V).

Functionally, phosphatases counteract the actions of protein kinases by catalyzing the removal of phosphate groups, thus placing them in the path of very important physiological processes. They are involved in the regulation of such cellular processes as mitosis, cell proliferation and differentiation, cell signaling, and metabolism (1,2). Phosphoprotein phosphatases are classified as multifunctional if they catalyze the dephosphorylation of several substrates or as specific phosphoprotein phosphatases if they act only on a specific substrate (3). Other criteria that have been used to classify phosphatases include pH optimum, size, type of substrate, substrate specificity, and the enzyme phosphoryl acceptor (2,4–8). More recently, however, amino acid sequence homology and sequence motifs that determine phosphatase activity have been used to group the phosphatases (5,6,9). The protein tyrosine phosphatase family, for instance, is characterized by the (I/V)HCXAGXGR(S/T) motif; the serine/threonine protein phosphatases by the DXH(X<sub>~25</sub>)GDXX(X<sub>~25</sub>)GNH(D/E) motif; phosphoglycerate mutase, 6-phosphofructo-2-kinase/fructose-2,6-bisphosphatase and several acid phosphatases by the

<sup>†</sup>Supported by NIH Grant GM62120. M.I.N. is a UNCF/Pfizer Fellow. M.E. was supported by a postdoctoral fellowship from the Swedish Natural Science Research Council.

\*To whom correspondence should be addressed. E-mail: craig.crews@yale.edu.

<sup>‡</sup>These authors contributed equally to this study.

<sup>||</sup>Present address: Department of Organic Chemistry, Umeå University, SE-901 87 Umeå, Sweden.

RHG motif; the family of glucose-6-phosphatases, nonspecific acid phosphatases, and several lipid phosphatases by a complex motif that consists of the sequence KX6RP(X<sub>12-54</sub>)PSGH (X<sub>31-54</sub>)SRX5-HX3D; phosphoserine phosphatase, phosphomannomutase, and several phosphotransferases by the DXDX(T/V) motif (2,6,10–12).

In general, protein phosphatases act in concert with kinases (13,14). The diversity of kinases and their involvement in controlling a variety of cellular responses to external stimuli have made them excellent targets for the development of new drugs (15–18). As such, we have previously shown that the antiinflammatory sesquiterpene lactone parthenolide disrupts the cytokine-induced proinflammatory NF- $\kappa$ B<sup>1</sup>-mediated signaling pathway by inhibiting IKK $\beta$ , the most critical component of the I kappa B kinase (IKK) complex for this process (19). In an attempt to determine additional targets of parthenolide, a 34 kDa protein was identified as a major biotinylated protein in lysates from biotinylated parthenolide-treated EL4 cells. Pretreatment with excess parthenolide, before challenging EL4 cells with biotinylated parthenolide, resulted in the loss of the biotinylated p34. Biochemical and site-directed mutagenesis data suggest that p34 is a phosphatase of the family that utilizes aspartic acid as their nucleophile (9,11,20). In both in vitro and in vivo experiments, biotinylated parthenolide bound to p34 but had no effect on its enzymatic activity, suggesting that the binding sites for parthenolide were different from the active site of the enzyme. Additionally, overexpression of p34 did not have any effect on TNF- $\alpha$ -induced NF- $\kappa$ B DNA binding activity.

While the physiological role of p34 and the relevance of p34 as a target of parthenolide have yet to be determined, the present characterization using *p*NPP as a model substrate will aid in the elucidation of this protein's intracellular role.

## MATERIALS AND METHODS

### Purification of p34

To identify the 34 kDa parthenolide binding protein (p34), a large-scale purification scheme was designed. Twenty liters of murine lymphoma EL4 cells in the form of a harvested cell pellet was obtained from the National Cell Culture Center (Minneapolis, MN). Cell pellets were resuspended in 300 mL of RPMI 1640 medium (Gibco-BRL) with 5% calf serum and incubated with 4  $\mu$ M biotinylated parthenolide (19) for 2 h. Cells were harvested, washed in phosphate-buffered saline, and then Dounce homogenized in hypotonic lysis buffer [10 mM Hepes, pH 7.9, 10 mM NaCl, and 3 mM MgCl<sub>2</sub>], plus freshly added protease inhibitors (5  $\mu$ g/mL aprotinin, 10  $\mu$ g/mL leupeptin, 10  $\mu$ g/mL pepstatin, and 0.1 mM PMSF)]. The cell lysate was spun at 100000g at 4 °C for 5 h. The supernatant (S100) was then batch adsorbed onto an anion-exchange (DE52) resin and eluted with 100 mM NaCl. The eluant was diluted 5-fold in 25 mM MES buffer (pH 5.7). SP-Sepharose Fast Flow (SPFF) cation-exchange resin was added and the suspension rocked for 30 min. The mixture was filtered (using 0.2  $\mu$ m membrane) and incubated with 500  $\mu$ L of immobilized NeutrAvidin (Pierce) beads at 4 °C overnight. The beads were then collected and extensively washed sequentially under 1 M NaCl, extreme pH (2.8 and 11), and 0.1% Triton X-100 conditions. Reducing SDS-PAGE loading buffer (with 2% SDS) was added, and the beads were boiled for 20 min to release biotinylated proteins. Proteins were then resolved by 12% SDS-PAGE and stained with Coomassie blue or analyzed by Western blot.

<sup>1</sup>Abbreviations: EE-epitope, NH<sub>2</sub>-EYMPME-COOH; EDTA, ethylenediaminetetraacetic acid; *p*NPP, *p*-nitrophenyl phosphate; *p*NPPase, *p*-nitrophenyl phosphatase; P<sub>i</sub>, inorganic phosphate; IKK $\beta$ , I $\kappa$ B kinase beta; NF- $\kappa$ B, nuclear factor kappa B; PCR, polymerase chain reaction; GST, glutathione *S*-transferase; MALDI, matrix-assisted laser desorption ionization; RP-HPLC, reverse-phase high-pressure liquid chromatography; EST, expressed sequence tag; HRP, horseradish peroxidase; PMSF, phenylmethanesulfonyl fluoride; PSI-BLAST, position-specific iterative BLAST.

### Cloning and Expression of p34

Full-length cDNA of p34 was amplified from an EST clone (IMAGE no. 1511239) purchased from American Tissue Culture Center (ATCC) by polymerase chain reaction (PCR) using the following primers: 5'GCGAATTCACCATGGAATACATGCCAATG-GAAGAATACATGCCAATGGAAATGGCAGAGGCG-GAAGCCGG3' and 5'CGTTGCGGCCGCTTAACCTTGAA-GGGCAGGCAAGAG3'. The PCR product was digested with *NotI* and *EcoRI* and cloned into pcDNA3neo and pGEX-4T-1 to generate an EE-peptide-tagged epitope and a GST-tagged p34, respectively.

### Cell Culture/Transfection/Immunoprecipitation

HeLa M cells were maintained in Dulbecco's modified essential medium (DMEM) from Gibco BRL (Gaithersburg, MD) supplemented with 10% fetal bovine serum and antibiotics/antimycotics (100 units/mL penicillin, 100 µg/mL streptomycin, 1.25 µg/mL amphotericin B). Cells were transfected with the appropriate plasmid for 24 h using FuGENE 6 transfection reagent (Roche, Indianapolis, IN) before treatment with drug or vehicle (DMSO) for 1 h. Parthenolide was purchased from Sigma (St. Louis, MO) while biotin-parthenolide was synthesized as earlier described (19). For the in vivo inhibition experiment, cells were also treated with 20 ng/mL TNF- $\alpha$  (Roche). Cells were lysed in lysis buffer (20 mM HEPES/KOH, pH 7.9, 350 mM NaCl, 20% glycerol, 1% NP-40) to which protease inhibitors (0.1 mM PMSF, 10 µg/mL pepstatin, 10 µg/mL leupeptin, and 5 µg/mL aprotinin) had been freshly added and incubated with 2–5 µg of anti-EE-peptide antibody at 4 °C for 1 h. Protein G–Sepharose was then added and incubation continued for another 30–60 min. Immune complexes were washed three times with lysis buffer. After the last wash, residual buffer was removed from the beads, which were then prewarmed in a 37 °C water bath. One hundred microliters of the prewarmed reaction mixture (25 mM Tris-HCl, pH 7.8, 10 mM *p*NPP, 1 mM MgCl<sub>2</sub>, and 75 mM KCl; pH of final mixture was 7.6) was added, and the mixture was incubated for 15 min with occasional mixing. The reaction was stopped by addition of 1 M NaOH/0.1 M EDTA and mixing. The beads were spun down in a microcentrifuge, then 100 µL of the supernatant was transferred to a 96-well plate, and absorbance was determined at 405 nm.

### Enzyme Activity Assay

The reaction mixture for the determination of enzyme activity consists of 25 mM Tris-HCl, pH 7.8, 1 mM MgCl<sub>2</sub>, and 75 mM KCl. For the kinetic measurements, *p*NPP was used at concentrations of 0.25–12 mM, in a 100 µL volume. Enzyme (5 µL of a 10 nM solution) was added last and the absorbance determined at 405 nm in 96-well plates using a SpectraMax 250 (Molecular Devices, Sunnyvale, CA) plate reader. In end point measurements, the reaction was stopped after 15 min incubation by the addition of NaOH and EDTA to a final concentration of 0.5 and 0.05 M, respectively. All reactions were incubated at 37 °C. The effect of metal ions and phosphatase inhibitors was determined using 10 mM *p*NPP at pH 7.6. A molar extinction coefficient of 18330 M<sup>-1</sup> cm<sup>-1</sup> was used to determine the amount of *p*-nitrophenol released (21). Substrates other than *p*NPP were analyzed according to the method of Anner and Moosmayer (22), with slight modifications. MgCl<sub>2</sub>, KCl, and Tris-HCl buffer (at the same concentrations as already stated) were added to the substrate in a total volume of 69 µL, and the reaction was initiated by addition of 5 µL of enzyme (50 nM). After incubation at 37 °C for 45 min, 6 µL of H<sub>2</sub>SO<sub>4</sub> (24% v/w) was added, followed by 10 µL of 0.1 M ammonium molybdate and finally 10 µL of a coloring reagent [1% poly(vinyl alcohol) in 18.5 mg/100 mL Malachite Green]. The absorbance at 623 nm was read after 20 min incubation at room temperature. Blank readings were determined by substituting 5 µL of buffer for the enzyme.

## Site-Directed Mutagenesis

Site-directed mutagenesis was performed with the QuickChange site-directed mutagenesis system (QCM) from Stratagene (La Jolla, CA). In brief, a pair of synthetic oligonucleotide primers containing the desired mutations was used to amplify the supercoiled double-stranded DNA (dsDNA) plasmid with the insert of interest, in a single PCR reaction. The primers, each complementary to opposite strands of the vector, were extended using *pfu* DNA polymerase. The PCR product was then digested with *DpnI* to remove parental DNA and transformed into *Escherichia coli*. The primers used were as follows: forward, 5' ACGCTGCTGTTCAACTGCAATG-GCGTGCTGTGG3', and reverse, 5' CCACAGCACGCCAT-TGCAGTTGAACAGCAGCGT3', where the underlined residues indicate mutant residues. The mutations also resulted in the introduction of a novel *BsrDI* restriction site for rapid screening of mutant clones. All mutants were further confirmed by DNA sequencing.

## RESULTS

### Identification/Purification of a Putative Protein Phosphatase

In an effort to identify the intracellular molecular targets of parthenolide, a technique similar to that used in identifying fumagillin and eponemycin binding proteins (23–26) was employed. A murine lymphoma cell line (EL4) in log growth phase was treated with 2–4  $\mu$ M biotinylated parthenolide for 2 h with or without pretreatment with a 10-fold excess of parthenolide for 30 min. After being washed with PBS, the cells were lysed, and crude cellular lysates were resolved by SDS–PAGE followed by Western blotting analysis. Biotin-labeled proteins were visualized using streptavidin–horseradish peroxidase (SA–HRP) and enhanced chemiluminescence (ECL). Several bands appeared to be bound by biotinylated parthenolide (data not shown). However, two bands of molecular size 34 and 70 kDa were consistently competed away by pretreatment with excess parthenolide (data not shown). Our initial focus was on the 34 kDa band.

As a first step toward characterizing this parthenolide binding protein, DE52 and SP-Sepharose Fast Flow were investigated for their potential in the purification of p34. Biotinylated proteins in samples from each step of this partial purification were visualized using SA–HRP and ECL (Figure 1). After a final purification step using avidin–agarose, the purified 34 kDa band was excised from a SDS–polyacrylamide gel and analyzed by tryptic digestion followed by MALDI mass spectrometry.

Comparison of the mass spectrometry data with GenBank failed to match p34 with any known protein. Therefore, an alternative approach using peptide microsequence analysis was performed. Edman degradation of two RP-HPLC-purified tryptic peptides and comparison of the translated nucleotide database revealed that both sequences matched a murine-expressed sequence tag (EST) that has not been previously characterized. The full-length cDNA sequence was obtained by PCR amplification of the corresponding EST clone. PSI-BLAST analysis (27) of the cloned full-length sequence revealed that p34 belongs to a large family of hydrolases that includes L-2-haloacid dehalogenase, epoxide hydrolases, and phosphatases. The analysis also indicates that p34 is well conserved among eukaryotic species with the highest homology to human. Most of these protein homologues have not been characterized. p34 shares significant sequence similarity with *Saccharomyces cerevisiae* and *Schizosaccharomyces pombe* alkaline phosphatases PHO13 and PHO2, respectively (28,29). They have been previously designated *p*-nitrophenyl phosphatases. On the basis of these similarities and recent results showing that PHO13 has phosphatase activity against phosphorylated histone II-A and phosphorylated casein (30), p34 was presumed to be a putative protein phosphatase.

## Substrate Specificity

The possibility that p34 is a phosphatase was tested using *p*NPP as substrate. Incubation of purified GST-p34 with *p*NPP under alkaline conditions at 37 °C produced the characteristic yellow color, indicating hydrolysis of *p*NPP to *p*-nitrophenol and  $P_i$ . To determine the optimal conditions for this reaction, kinetic parameters were measured at various pH and substrate concentrations. Tris-HCl was used as buffer over the pH range 7.1–8.9. To determine the initial rate reactions, the amount of *p*-nitrophenol produced over a short period of time was measured at different *p*NPP concentrations. The maximum velocity was plotted using both the direct and the Lineweaver-Burk methods (Figure 3A,B). The initial rate measurement was very slow in the absence of  $Mg^{2+}$ ; hence, 1 mM  $MgCl_2$ , which approximates physiological  $Mg^{2+}$  concentration (31), was added to the reaction mixture. By plotting the log of maximum velocities against the actual pH of the reaction mixtures, the optimum pH was determined to be 7.6 over the pH range tested (Figure 3C). Above pH 7.6, the activity of the enzyme declined gradually in contrast to activity at pH values below 7.6. The  $K_m$  and  $K_{cat}$  values at the optimum pH were 1.36 mM and  $0.052 \text{ min}^{-1}$ , respectively. As summarized in Table 1, p34 showed fairly strong enzymatic activity toward  $\beta$ -glycerophosphate.

## Requirement for Metal Ions

Both monovalent and divalent cations have been shown to influence the activity of phosphatases (5,32,33). We first tested  $Mg^{2+}$  for its effect on *p*NPPase activity of p34. As shown in Figure 4A,  $Mg^{2+}$  had a strong activating effect, which extended up to 20 mM. We next tested the effect of  $Ca^{2+}$ ,  $Mg^{2+}$ ,  $Mn^{2+}$ ,  $Co^{2+}$ ,  $Cu^{2+}$ ,  $Zn^{2+}$ ,  $Fe^{2+}$ ,  $Na^+$ , and  $K^+$  at four different concentrations on the activity of p34.  $Ca^{2+}$ ,  $Cu^{2+}$ , and  $Zn^{2+}$  had no effect on the enzyme's activity while  $Co^{2+}$ ,  $Mg^{2+}$ , and  $Mn^{2+}$  stimulated the activity of p34 by 4 to 44-fold depending on the ion and concentration used (Figure 4B). In contrast to their inhibitory effects on yeast *p*NPPase activity (33),  $Na^+$  and  $K^+$  stimulated p34 *p*NPP hydrolysis activity (Figure 4C). The maximum effects were observed as 50 mM for  $Na^+$  and 75 mM for  $K^+$ . Above these concentrations, the presence of either ion in the reaction mixture inhibited enzyme activity.

## Effect of Known Phosphatase Inhibitors on p34

The effect of various known phosphatase inhibitors was determined at 37 °C using 10 mM *p*NPP, 1 mM  $Mg^{2+}$ , and 75 mM KCl at pH 7.6 in the presence of increasing concentrations of inhibitors. Figure 5A,B shows that neither sodium fluoride nor okadaic acid had any effect on p34 at concentrations that have been demonstrated to inhibit phosphatase activity (34). Sodium vanadate, on the other hand, inhibited enzyme activity by more than 50% at 100  $\mu$ M.

## Parthenolide Binds to p34 but Does Not Inhibit Its Activity

Since p34 was first identified and purified on the basis of its binding to biotinylated parthenolide, it was desirable to verify the effect of parthenolide and its biotinylated derivative on p34 activity. In an in vitro assay, purified GST-p34 (1  $\mu$ g) was treated with 20  $\mu$ M parthenolide or biotin-parthenolide in 25 mM Tris-HCl buffer, pH 7.8, for 1 h before the addition of substrate (10 mM *p*NPP). After a 30 min incubation at 37 °C, the reaction was stopped by the addition of NaOH at a final concentration of 0.5 M and the absorbance read at 405 nm. As a control, Tris-HCl buffer or the vehicle alone (DMSO) was added instead of the drug. Neither parthenolide nor biotin-parthenolide inhibited the activity of the enzyme (Figure 6A). Binding of biotin-parthenolide to p34 was verified by Western blotting using streptavidin-HRP in a duplicate reaction (data not shown).

The effect of parthenolide on p34 was also tested in an in vivo experiment. HeLa M cells were transfected with EE-epitope-tagged p34 and pretreated with 20  $\mu$ M parthenolide for 1 h, followed by 20 ng/mL treatment with TNF- $\alpha$  for various time intervals. The EE-epitope is a



six amino acid sequence (NH<sub>2</sub>-EYMPME-COOH) that was appended to the N-terminus of p34 to facilitate the purification of p34 from cell lysates. Recombinant p34 was immunoprecipitated from whole cell lysate and assayed for enzymatic activity. Figure 6B shows that enzymatic activity was not inhibited by parthenolide.

Examination of the amino acid sequence of p34 did not reveal the presence of the consensus motif [(H/V)C(X<sub>5</sub>)R-(S/T)] present in several protein tyrosine phosphatases (1,13,34). However, a large family of phosphatases is characterized by short sequence motifs that feature two aspartic acid residues separated by a single amino acid. Both residues are required for activity (9,11). Interestingly, a closer examination of the sequence alignment in Figure 2A revealed the presence of two aspartate residues (identified with asterisks) that are conserved in all of the aligned sequences. To determine the role, if any, played by these aspartate residues, site-directed mutagenesis was used to mutate them to asparagine. Both wild-type and mutant proteins were then overexpressed in HeLa M cells, immunoprecipitated with anti-EE-peptide monoclonal antibody, and assayed for enzyme activity. Figure 6C shows that the D34/36N mutant had no activity compared to the wild type.

The inability of parthenolide or biotin–parthenolide to inhibit the enzymatic activity of p34 in the in vivo and in vitro assays as shown in panels A and B of Figure 6 suggested that the binding site was different from the active site. This was further verified in Figure 6D whereby wt p34 and the enzymatically inactive mutant D34/36N bind equally strongly to biotin–parthenolide.

### Effect of p34 on TNF- $\alpha$ -Induced NF- $\kappa$ B DNA Binding Activity

Although the physiological substrate of p34 is yet to be determined, on the basis of the binding of p34 to parthenolide, we investigated a possible role for p34 in the proinflammatory signaling pathway. HEK 293 cells stably transfected with p34 were treated for various time intervals with TNF- $\alpha$  and assayed for NF- $\kappa$ B DNA binding activity using the electrophoretic mobility shift assay (EMSA) as readout. Figure 7 shows that the DNA binding activity in p34 stable transfectants is indistinguishable from that of normal HEK 293 cells, indicating that p34 is not likely involved in this pathway.

## DISCUSSION

A rapidly growing area of research is the use of modified small molecules and their analogues as probes in the elucidation of intracellular signaling pathways (25,35–37). For instance, the identification of the molecular targets of the anti-angiogenic compound fumagillin (38), the proteasome inhibitors epoxomicin and eponemycin (23,24,26), and specific substrates for Src kinases (39) was achieved through the use of modified biologically active small molecules. Using similar techniques we have identified and characterized p34, a putative protein phosphatase that binds to biotin–parthenolide, during a search for the intracellular molecular targets of parthenolide, an antiinflammatory agent. Initial comparison of the MALDI mass spectrometric data from p34 with the gene database revealed no matches to any known proteins. Further analysis by Edman degradation of two RP-HPLC-purified peptides identified a previously uncharacterized murine-expressed sequence tag (EST). The possibility that p34 was a protein phosphatase was suggested by the close sequence similarity between the translated EST and the yeast alkaline phosphatases PHO13 and PHO2 from *S. cerevisiae* and *S. pombe*, respectively. To provide evidence for this possibility, the kinetic parameters of p34 using *p*NPP as substrate were determined. We demonstrate that p34 catalyzes the hydrolysis of *p*NPP at an optimum pH of 7.6 and  $K_m$  and  $K_{cat}$  values of 1.36 mM and 0.052 min<sup>-1</sup>, respectively. However, while the easy readout and applicability to a wide range of pH conditions have been generally exploited in using *p*NPP as a substrate, Sparks and Brautigan (14,40) point out that the use of *p*NPP hydrolysis alone to designate a novel protein as a phosphatase could be misleading. Thus, we have employed other criteria such as cofactor

requirements, effects of known inhibitors, and the presence of sequence motifs to corroborate the *p*NPP hydrolysis data.

Our results show that p34 has little or no activity in the absence of  $Mg^{2+}$ , similar to the recently identified phosphatase MDP-1, which also employs the same characteristic DXDX(T/V) motif as its active nucleophile (5). In addition, the effects of other divalent and monovalent cations were tested. Similar results whereby some divalent cations are activating and others inhibitory have been observed with other phosphatases (5,32,33). Although p34 and PHO13 were similar in their amino acid sequence, they are differentially affected by  $Na^+$  and  $K^+$ . Unlike their inhibitory effect on PHO13, both  $Na^+$  and  $K^+$  activated p34.

Efforts have been made to characterize phosphatases on the basis of structural motifs that comprise their active sites (1,6,11,12,20). At least four groups of phosphatases have been classified using these criteria. One group, comprising the haloacid dehalogenases and other phosphotransferases, is characterized by the DXDX(T/V) motif in their amino-terminal region (9,11,20). By sequence alignment (Figure 2A) we show that p34 belongs to this group. Mutations in which either of the two aspartic acid residues in phospho-glucosyltransferase were changed to asparagine result in inactivation of the enzyme (11). Introduction of analogous mutations in p34 by site-directed mutagenesis, (D34/36N), abolished its enzyme activity.

Given that p34 was identified on the basis of its affinity for parthenolide, it was necessary to determine the effect of parthenolide on p34. Parthenolide did not have any observable effect on the hydrolysis of *p*NPP by p34 in either the in vitro or in vivo model inhibition assays. The binding of parthenolide to p34 was however unaffected in either case, suggesting that the active site and the parthenolide binding site(s) are different. Therefore, it is possible that p34 is a parthenolide binding protein with no physiological relevance to the actions of parthenolide as an antiinflammatory agent. Determination of the natural substrate(s) for p34 may help to validate this idea.

IKK $\beta$  plays a major role in the NF- $\kappa$ B-mediated proinflammatory process by phosphorylating I $\kappa$ B (a cytoplasmic inhibitor of NF- $\kappa$ B), which then is ubiquitinated and subsequently degraded via the proteasome (15). The phosphorylation, ubiquitination, and degradation of I $\kappa$ B is a prerequisite for NF- $\kappa$ B entry into the nucleus and activation of transcription. Recently, we showed that parthenolide interferes with this signaling pathway by inhibiting the phosphorylation of I $\kappa$ B by I $\kappa$ B kinase, IKK $\beta$  (19). IKK $\beta$  is part of a large multicomplex protein whose components have not been fully determined (16–18). It might be mere coincidence that parthenolide binds to IKK $\beta$  (a kinase) and p34 (a phosphatase), since the current EMSA results do not suggest the involvement of p34 in NF- $\kappa$ B signaling. Other than its direct inhibitory effect on inflammation through IKK $\beta$  parthenolide could possibly have other yet unidentified physiological effects that may be mediated through p34. Conceivably, p34 might also have functions other than its phosphatase activity that are influenced by parthenolide. Issues such as these are easily addressable when the natural substrate for p34 is identified. Incidentally, the medicinal herb Feverfew (*Tanacetum parthenium*) from which parthenolide is derived has been used not only for its antiinflammatory properties but also in treating migraine headaches and rheumatoid arthritis (41–43). One or more these effects could be mediated through p34.

While the physiological significance of the binding of parthenolide to p34, a phosphatase, is currently unknown, the characterization in this paper and the verifiable possibilities raised will hopefully provide a starting point for further investigation of this protein.

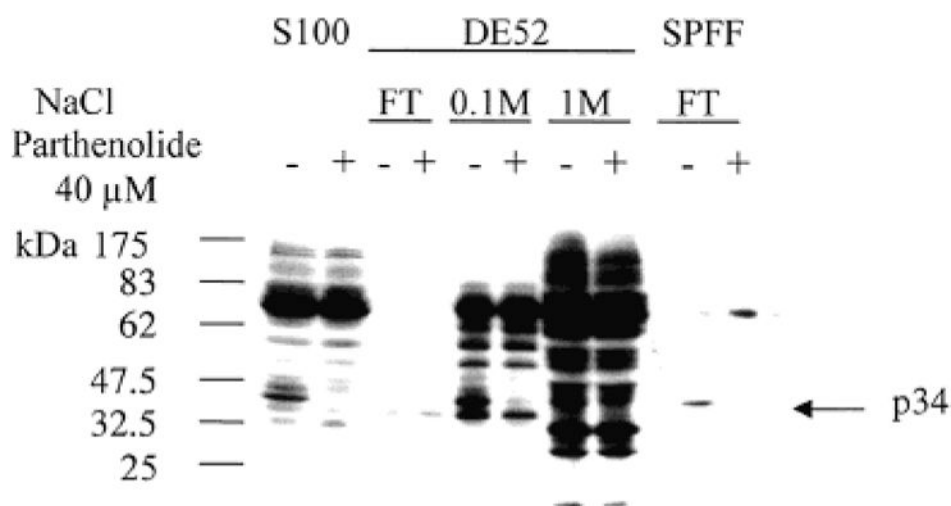
## REFERENCES

1. Peters GH, Frimurer TM, Olsen OH. Biochemistry 1998;37:5383–5393. [PubMed: 9548920]
2. Stone RL, Dixon JE. J. Biol. Chem 1994;269:31323–31326. [PubMed: 7989293]

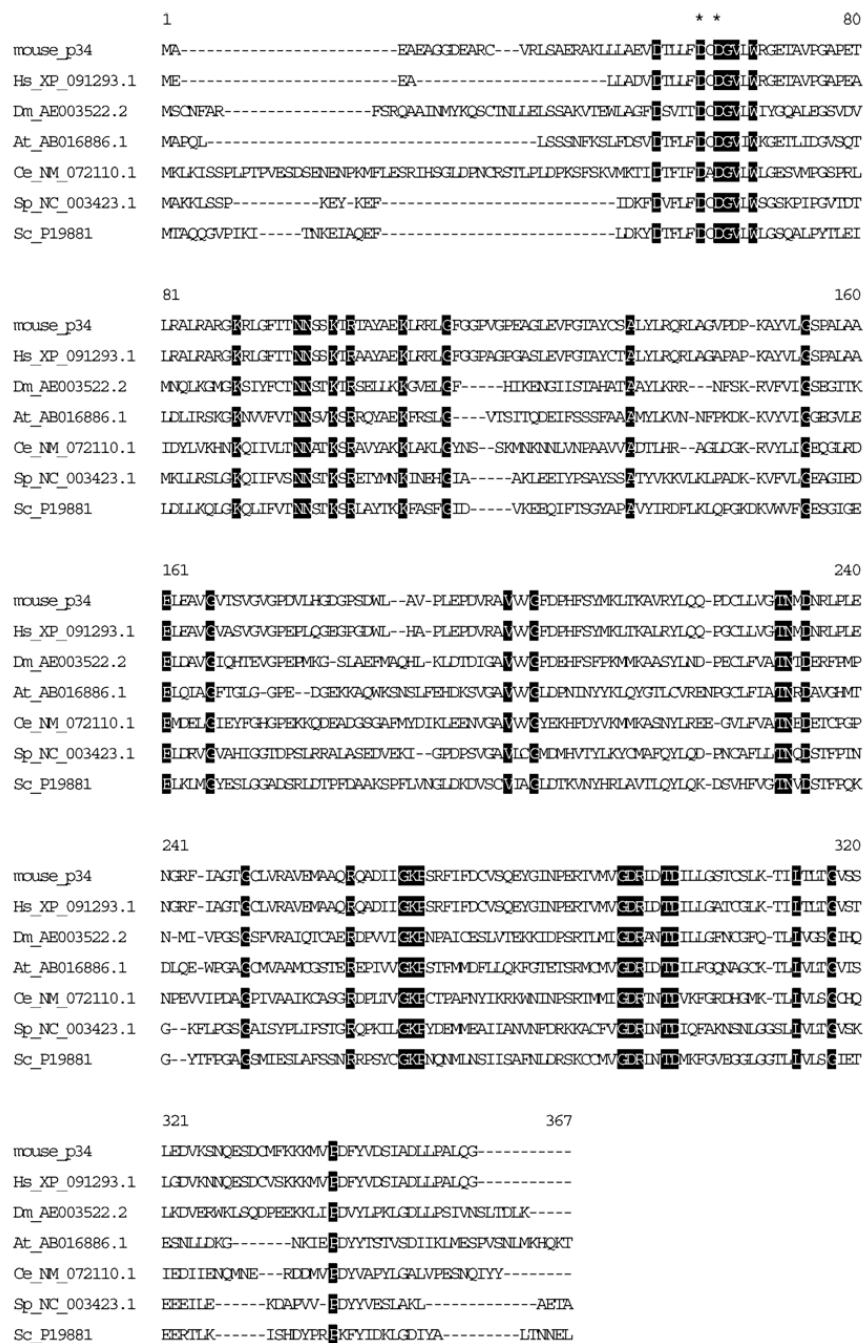
3. Krebs EG, Beavo JA. *Annu. Rev. Biochem* 1979;48:923–959. [PubMed: 38740]
4. Boyer, PD.; Lardy, H.; Mayback, K., editors. *The Enzymes*. Vol. V. New York: Academic Press; 1961.
5. Selengut JD, Levine RL. *Biochemistry* 2000;39:8315–8324. [PubMed: 10889041]
6. Stukey J, Carman GM. *Protein Sci* 1997;6:469–472. [PubMed: 9041652]
7. Vincent JB, Crowder MW, Averill BA. *Trends Biochem. Sci* 1992;17:105–110. [PubMed: 1412693]
8. Walsh, C. *Enzymatic Reaction Mechanisms*. New York: W. H. Freeman and Co; 1979.
9. Collet JF, Stroobant V, van Schaftingen E. *J. Biol. Chem* 1999;274:33985–33990. [PubMed: 10567362]
10. Bazan JF, Fletterick RJ, Pilgis SJ. *Proc. Natl. Acad. Sci. U.S.A* 1989;86:9642–9646. [PubMed: 2557623]
11. Collet JF, Stroobant V, Pirard M, Delpierre G, van Schaftingen E. *J. Biol. Chem* 1998;273:14107–14112. [PubMed: 9603909]
12. Zhuo S, Clemens JC, Stone RL, Dixon JE. *J. Biol. Chem* 1994;269:26234–26238. [PubMed: 7929339]
13. Chengalvala MV, Bapat AR, Hurlburt WW, Kostek B, Gonder DS, Mastroeni RA, Frail DE. *Biochemistry* 2001;40:814–821. [PubMed: 11170399]
14. Sparks JW, Brautigan DL. *Int. J. Biochem* 1986;18:497–504. [PubMed: 3011539]
15. Ghosh S, May MJ, Kopp EB. *Annu. Rev. Immunol* 1998;16:225–260. [PubMed: 9597130]
16. Maniatis T. *Science* 1997;278:818–819. [PubMed: 9381193]
17. Rothwarf DM, Zandi E, Natoli G, Karin M. *Nature* 1998;395:297–300. [PubMed: 9751060]
18. Yamaoka S, Courtois G, Bessia C, Whiteside ST, Weil R, Agou F, Kirk HE, Kay RJ, Israel A. *Cell* 1998;93:1231–1240. [PubMed: 9657155]
19. Kwok BH, Koh B, Ndubuisi MI, Elofsson M, Crews CM. *Chem. Biol* 2001;8:759–766. [PubMed: 11514225]
20. Ridder IS, Dijkstra BW. *Biochem. J* 1999;339:223–226. [PubMed: 10191250]
21. Biggs AI. *Trans. Faraday Soc* 1954;50:800–802.
22. Anner B, Moosmayer M. *Anal. Biochem* 1975;65:305–309. [PubMed: 1130683]
23. Meng L, Kwok BH, Sin N, Crews CM. *Cancer Res* 1999;59:2798–2801. [PubMed: 10383134]
24. Meng L, Mohan R, Kwok BH, Elofsson M, Sin N, Crews CM. *Proc. Natl. Acad. Sci. U.S.A* 1999;96:10403–10408. [PubMed: 10468620]
25. Sin N, Kim KB, Elofsson M, Meng L, Auth H, Kwok BH, Crews CM. *Bioorg. Med. Chem. Lett* 1999;9:2283–2288. [PubMed: 10465562]
26. Sin N, Meng L, Auth H, Crews CM. *Bioorg. Med. Chem* 1998;6:1209–1217. [PubMed: 9784862]
27. Galperin MY, Bairoch A, Koonin EV. *Protein Sci* 1998;7:1829–1835. [PubMed: 10082381]
28. Kaneko Y, Toh-e A, Banno I, Oshima Y. *Mol. Gen. Genet* 1989;220:133–139. [PubMed: 2558283]
29. Yang JW, Dhamija SS, Schweingruber ME. *Eur. J. Biochem* 1991;198:493–497. [PubMed: 1645660]
30. Tuleva B, Vasileva-Tonkova E, Galabova D. *FEMS Microbiol. Lett* 1998;161:139–144. [PubMed: 9561742]
31. Alberts, B.; Bray, D.; Lewis, J.; Raff, M.; Roberts, K.; Watson, JD. *Molecular Biology of The Cell*. 3rd ed. New York and London: Garland Publishing; 1994.
32. Attias J, Bonnet JL. *Biochim. Biophys. Acta* 1972;268:422–430. [PubMed: 4554643]
33. Attias J, Durand H. *Biochim. Biophys. Acta* 1973;321:561–568. [PubMed: 4357666]
34. Grangeasse C, Doublet P, Vincent C, Vaganay E, Riberty M, Duclos B, Cozzzone AJ. *J. Mol. Biol* 1998;278:339–347. [PubMed: 9571056]
35. Bishop A, Buzko O, Heyeck-Dumas S, Jung I, Kraybill B, Liu Y, Shah K, Ulrich S, Witucki L, Yang F, Zhang C, Shokat KM. *Annu. Rev Biophys. Biomol. Struct* 2000;29:577–606. [PubMed: 10940260]
36. Crews CM, Mohan R. *Curr. Opin. Chem. Biol* 2000;4:47–53. [PubMed: 10679374]
37. Elofsson M, Splittgerber U, Myung J, Mohan R, Crews CM. *Chem. Biol* 1999;6:811–822. [PubMed: 10574782]
38. Sin N, Meng L, Wang MQ, Wen JJ, Bornmann WG, Crews CM. *Proc. Natl. Acad. Sci. U.S.A* 1997;94:6099–6103. [PubMed: 9177176]



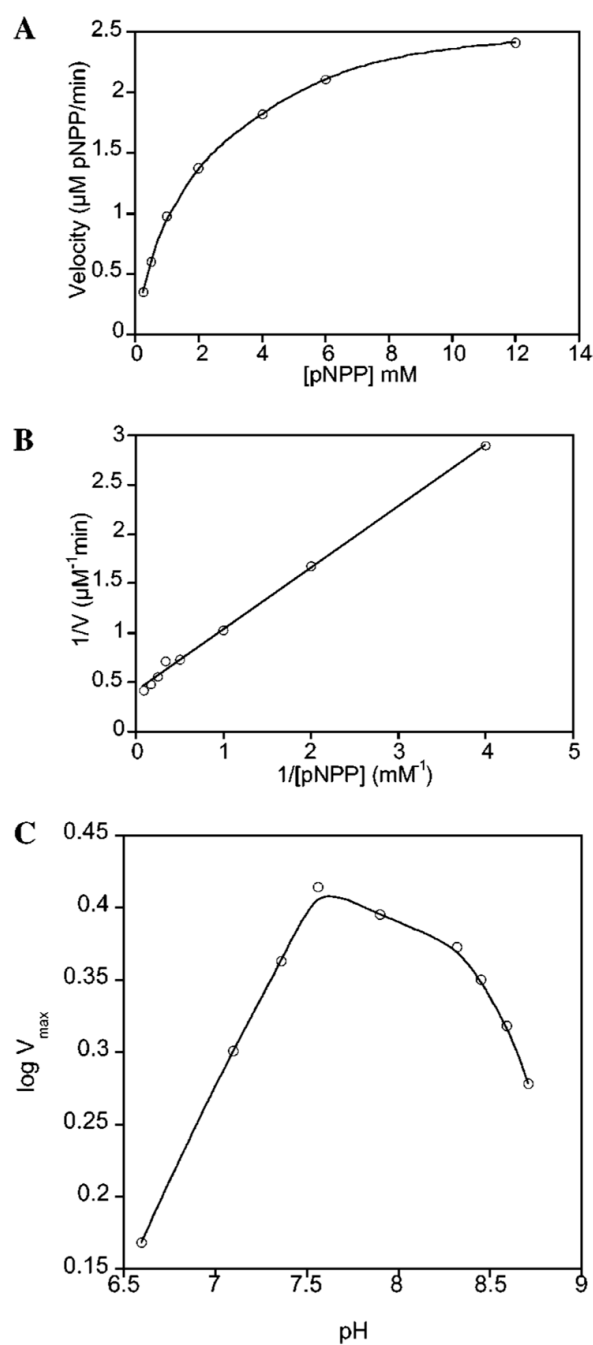
39. Shah K, Liu Y, Deirmengian C, Shokat KM. Proc. Natl. Acad. Sci. U.S.A 1997;94:3565–3570. [PubMed: 9108016]
40. Sparks JW, Brautigan DL. J. Biol. Chem 1985;260:2042–2045. [PubMed: 2982803]
41. Ernst E, Pittler MH. Public Health Nutr 2000;3:509–514. [PubMed: 11276299]
42. Patrick M, Heptinstall S, Doherty M. Ann. Rheum. Dis 1989;48:547–549. [PubMed: 2673080]
43. Pittler MH, Vogler BK, Ernst E. Cochrane Database Syst. Rev 2000;3

**FIGURE 1.**

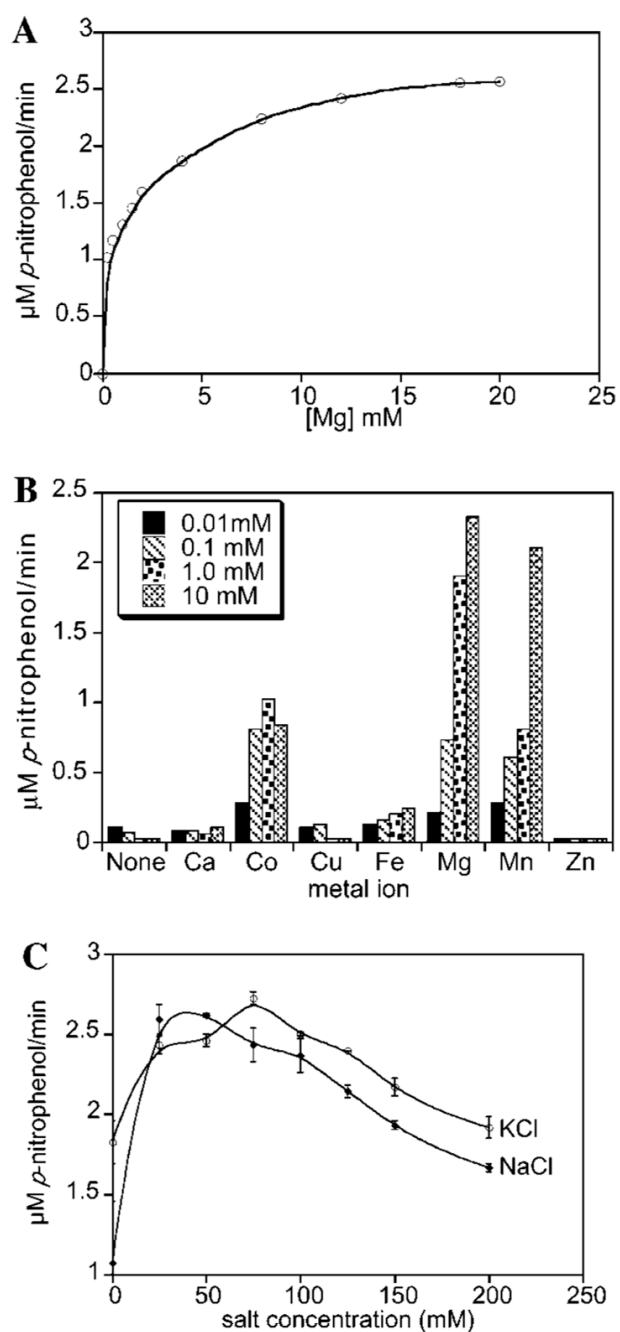
Affinity purification of p34. EL4 cells pretreated with or without 40  $\mu$ M parthenolide were labeled with 4  $\mu$ M biotinylated parthenolide. The cell lysate was sequentially purified by a 5 h 100000g centrifugation (S100) and DE52 and SP-Sepharose Fast Flow (SPFF) ion-exchange chromatography. An aliquot of sample from each step (FT is the flow through) was resolved by 12% SDS-PAGE and blotted with streptavidin-HRP.

**FIGURE 2.**

Sequence alignment of p34 with other phosphatases. The sequence of p34 is compared with *p*-nitrophenyl phosphatases from *Homo sapiens*, *Caenorhabditis elegans*, *Drosophila melanogaster*, *A. thaliana*, *S. pombe*, and *S. cerevisiae* using PSI-BLAST search analysis. The sequences were aligned using the Meg Alignment program, and conserved amino acids are highlighted. Mutations of the two aspartate residues indicated with asterisks to asparagine abolished the *p*-nitrophenyl phosphatase activity of p34.

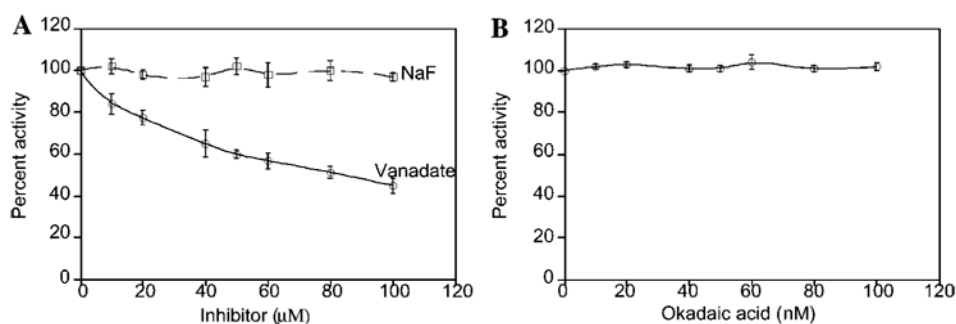
**FIGURE 3.**

(A) Plot of the initial velocities against substrate concentration to obtain a direct maximum velocity plot. (B) Maximum velocity determined by the indirect method of Lineweaver-Burk. (C) Effect of pH on the activity of p34.

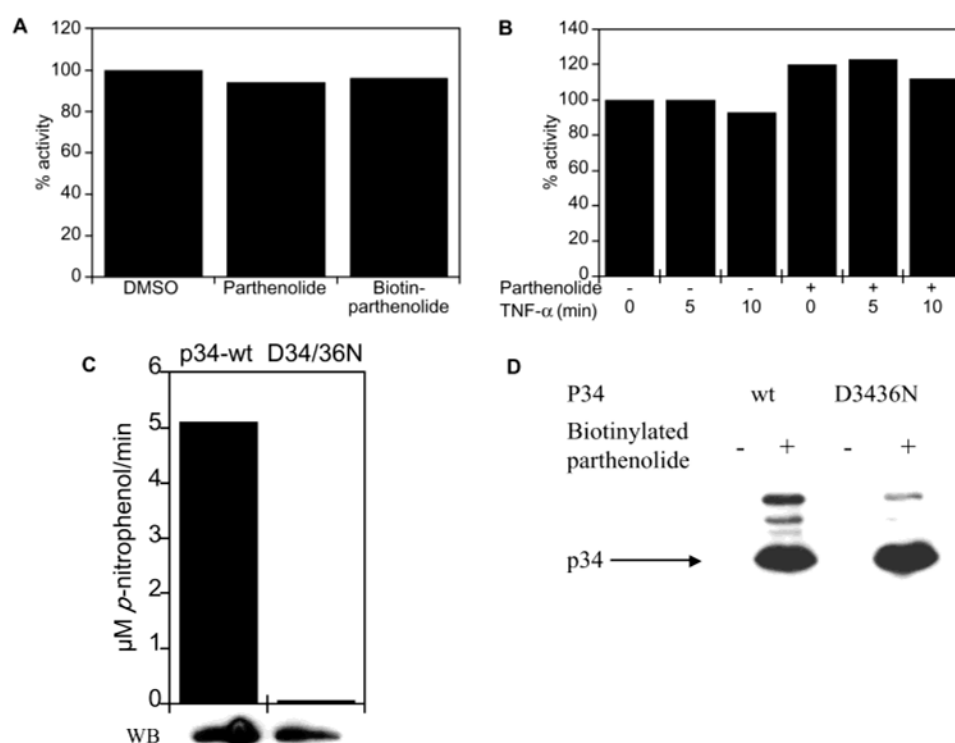
**FIGURE 4.**

Effect of divalent metal ions on the activity of p34. (A) Effect of  $\text{Mg}^{2+}$  ions on enzymatic activity. (B) Effect of increasing concentrations of different metal ions on enzymatic activity. (C) Effect of salt (KCl, NaCl) on enzymatic activity.



**FIGURE 5.**

Effect of phosphatase inhibitors. The effect of various known phosphatase inhibitors on p34 was tested. The phosphatase activity was determined as described for the enzyme assay in the presence of increasing concentrations of inhibitors. Results are expressed as percentage inhibition using the absence of inhibitor as 100% activity. (A) Sodium vanadate and sodium fluoride. (B) Okadaic acid.

**FIGURE 6.**

Parthenolide binds but does not inhibit p34. (A) In vitro inhibition assay. Purified GST-p34 treated with parthenolide or biotinylated parthenolide was tested for *p*NPP activity. Untreated and DMSO-treated cells served as control. In vitro binding of biotinylated parthenolide was verified by Western blotting using streptavidin-HRP (data not shown). (B) HeLa M cells transfected with EE-epitope-tagged wt p34 were pretreated with parthenolide for 1 h followed by 10 ng/mL TNF- $\alpha$  for various time intervals. Cell lysates were immunoprecipitated with anti-EE peptide antibody and tested for *p*NPP activity. Cells treated for the same time interval with TNF- $\alpha$  but without parthenolide pretreatment were used as control. (C) Same as in (B) but without parthenolide or TNF- $\alpha$  treatment. Mutation of aspartate residues at positions 34 and 36 to asparagine abolished the *p*NPP activity. The Western blot confirming the presence of EE-peptide-tagged p34 in the immunoprecipitation is shown. (D) HeLa M cells transfected with wt p34 and the D34/36N mutant were immunoprecipitated with anti-EE peptide antibody and visualized by streptavidin-HRP and enhanced chemiluminescence.

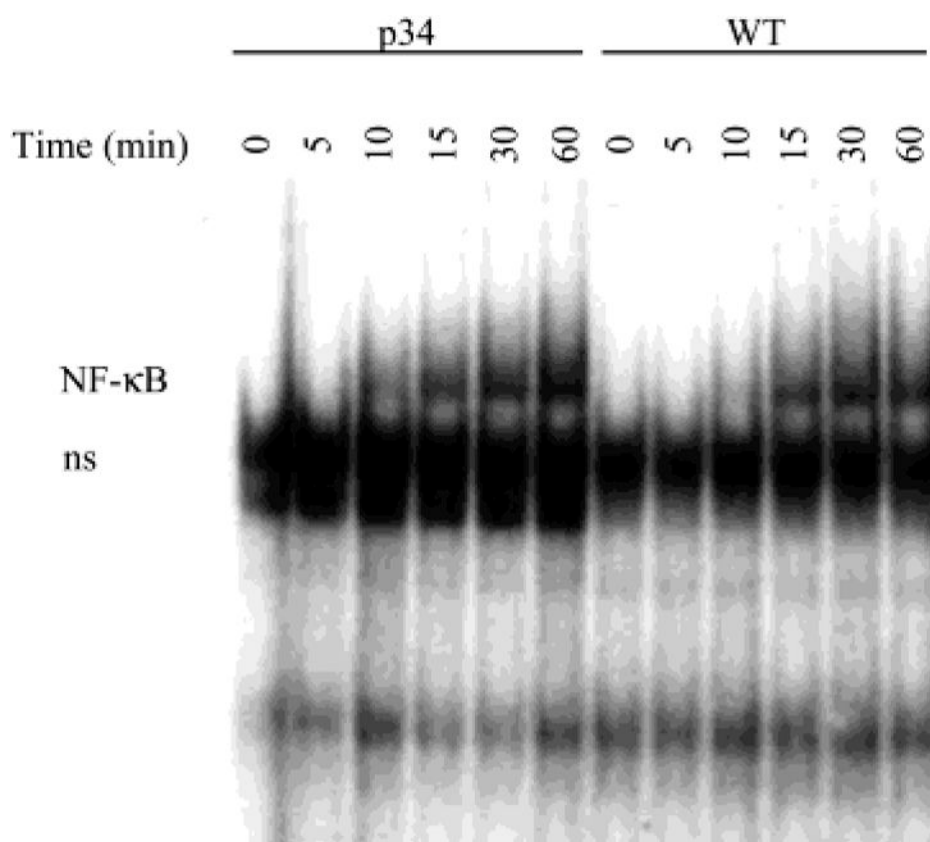


**FIGURE 7.**

p34 overexpression has no effect on TNF- $\alpha$ -induced NF- $\kappa$ B DNA binding activity. Cell lysates from normal HEK 293 and HEK 293 stably transfected with p34 induced with TNF- $\alpha$  (10 ng/mL) were analyzed using electrophoretic mobility shift assays (EMSA) for DNA binding activity. ns = nonspecific band.

**Table 1a**

| substrate | relative activity (%) | substrate                 | relative activity (%) |
|-----------|-----------------------|---------------------------|-----------------------|
| pNPP      | 100                   | $\beta$ -glycerophosphate | 53                    |
| ATP       | 0                     | creatine phosphate        | 8.5                   |
| AMP       | 4.9                   | casein                    | 7.4                   |

<sup>a</sup> Substrates were assayed at 5 mM. The amount of P<sub>i</sub> released was determined using an extinction coefficient of 99600 M<sup>-1</sup> cm<sup>-1</sup> (see ref 23). Casein was tested at 0.005%.